

TOWARDS INFLUENCES OF THE EPS ON LUNAR ROVER'S SYSTEMS DESIGN

Niklas A. Mulsov¹, Benjamin Huelsen¹, Patrick Schoeberl¹

¹ German Research Center for Artificial Intelligence (DFKI) - Robotics Innovation Center, Bremen, Germany
Email: {niklas.mulsov, benjamin.huelsen, patrick.schoeberl, }@dfki.de

ABSTRACT

In this paper, we describe the specification of the rover MOVE¹ with a mass of approximately 5 kg for lunar surface exploration, closely based on the development of the rover's Electrical Power System (EPS). Fundamental relations, such as the interaction of the Thermal Control System (TCS) and EPS on the performance of the rover, will be described. The rover design approach includes budgets for mass and power of the needed subsystems like On Board Computer (OBC), payload, radio, Vehicle Control Unit (VCU), Guidance Navigation and Control (GNC) and the arrangement and number of solar cells have been used. This makes the rover an ideal testbed for the performance of the EPS under realistic conditions. The described results are based on the DFKI's outcome of the project SEARCH², which ended in January 2022 and was a collaboration together with the Walter Kern GmbH.

Key words: Rover, Lunar, Electrical Power System, System Design, Energy, Supercapacitors.

1. INTRODUCTION

Related Work Research on robots and landing platforms for the exploration of the moon has started worldwide, especially since Google Lunar X-Prize brings more and more private companies and university teams on track. Figure 1 show promising competitors for the first micro rover to be landed on the lunar surface. These are for example the rovers HAKUTO from iSpace [1], the team Indus rover [2], MAPP from Lunar Outpost [3] and the CUBEROVER from Astrobotics [4]. However, until now no private team has landed successfully but it can be assumed that in future the opportunities to explore the moon will greatly expand. Interrelationships between energy storage technologies, system design and also with the TCS led us to think that, there is still potential in here to build capable rovers for lunar exploration.

¹MOon VEhicle

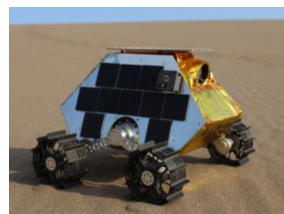
²<https://robotik.dfk-bremen.de/de/forschung/projekte/search/>



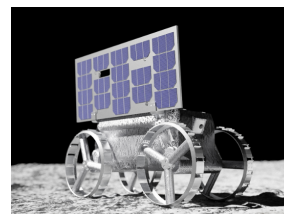
(a) HAKUTO, iSpace



(b) Rover from Team Indus



(c) MAPP, Lunar Outpost



(d) CUBEROVER, Astrobotics

Figure 1. Systems with envisaged landing in the mid of the 2020s

Objectives Envisaged operation time is planned for a 12 day mission during lunar day where the operation radius from lander is around 500 meters. Besides, the rover could serve as a scout for a larger system in a multirover scenario [5]. A nightsurvival has been ruled out because of technical capabilities for such a small system. However, it is considerable to realize this by a more powerful energy storage in a bigger system with a mass of over 15 kg like the MAPP Rover from Lunar Outpost [3].

2. DESIGN APPROACH

In an initial step, the power budgets for the subsystem were determined to specify basic requirements for the EPS. For this purpose, values of comparable systems and for usable subsystems from the cubesat market³ have been investigated. The power train properties, which have a major influence, were calculated from engine and gearbox manufacturer data. It is striking that the miniaturization leads to over-proportionally high power losses

³German Orbital Systems, ISISPACE, EnduroSat, AAC Clyde Space, Pumpkin

through the gearbox and motor drivers themselves. Reducing the power losses can be achieved by lowering the rotational speed through the wheel diameter or the rover speed itself. The reduction of the number of drives to two was also discussed, but rejected in favour of off-road capability and redundancy. However, these effects should not be underestimated. Table 1 showing estimated values for the SEARCH Rover.

Table 1. Power Budget and EPS requirements for the SEARCH Rover. The moving speed of the rover is 0.1 ms^{-1} . Values for OBC, CAM and Radio were derived from comparable space qualified components, ¹: with efficiency losses

Subsystem	Power.cont [W]	Power.max [W]
OBC	1.2	1.5
EPS ¹	1.0	1.0
Motors	4.5	17.7
Motor Controllers	4.4	4.4
VCU	2.8	2.8
Camera + Payload	1.7	3.7
Telemetry/Radio	1.0	1.7
Power.total.idle		7.0
Power.total.drive.cont		16.6
Power.total.drive.peak		28.4

To meet the power requirements, different storage technologies and the influences to the rovers system design were investigated. For this, the EPS is built modular and allows the integration of further subsystems, see section 3.2 and 3.1. The solar panels were initially designed to provide a non-stop operation of the rover. This approach allows to eliminate the need for chemical storage in the system which is also beneficial for lowering the needs for the TCS in cool environments. To accomplish this, the use of supercapacitors for the rover will be explored as an alternative storage technology.

For placing the solar cells, typically lunar rovers are closely aligned with the latitude of the landing site. During the daytime, there is generally a surplus of thermal energy that cannot be radiated in the direction of the heated lunar ground. To determine the position of the solar cells for calculating the aimed solar flux and electrical current, figure 2 show an overview of small lunar rovers equipped with passive TCS. As a result for an wide range of latitude of the landing site, a pyramid shape for the rovers body with an isolation to ground is advisable [6]. This comprise a always sun facing surface to harvest energy on the one hand and a slightly larger surface to the dark facing side on the other hand to dissipate surplus energy. A radiator on topside supports the system getting overheated. To take advantage of the energy dissipation of the dark facing solar array a thermal conductivity between sun facing and dark facing site is necessary.

To prove that assumption and confirming the placement of the solar cells, a thermal simulation of the rover was performed. The model used for it was separated into five physical bodies: wheels, chassis, main body, solar cells, and the electrical box inside. For the main body, different surfaces such as an MLI isolation to ground and different coatings for analysing various radiation parameters have

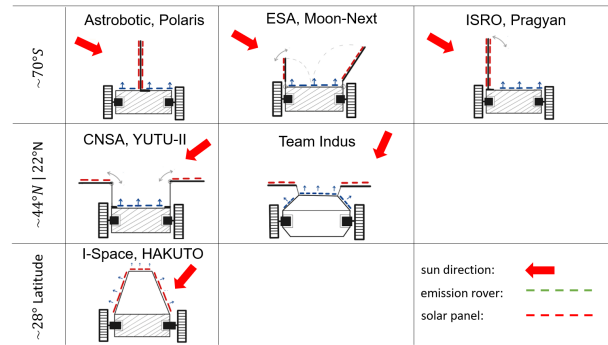
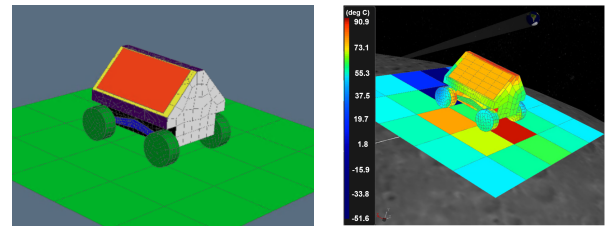


Figure 2. Rover body configuration of state of the art rovers depending from latitude of the landing site



(a) Simplified rover model for thermal simulation. *green*: wheels, *blue*: chassis, *black*: ground isolation, *violet*: radiation surfaces, *yellow*: solar cell mounting, *orange*: solar cells, *grey*: rover body

(b) Simulation of the model on lunar surface with Thermica v4. Because of the low thermal conductivity of the regolith and static modelling, strong shadows of the system can be seen on ground

been simulated. Figure 3(a) shows the model for the simulation without the electrical box inside. Thermal coupling parameters for the conductivity of the bodies was set by hand, respective to material and geometrical properties. Wheels and chassis were almost thermally decoupled from system. Figure 3(b) shows the result of the simulation for the first iteration of the rover.

It became apparent that with a rover body made from CFRP by a thickness of 2 mm the heat conductivity is not satisfying to distribute the heat in the rovers hull. This leads to temperatures from $+90 \text{ }^\circ\text{C}$ for the solar panels on the sun facing site and $-60 \text{ }^\circ\text{C}$ at the dark facing side. Therefore as body material aluminium was proved to reduce the temperature differences.

Results have been calculated after enlarging the rovers top site used as radiator by increasing the panels angle of the solar panels to 67° , using a white coating for the rovers side surfaces and connection the electronic compartment and radiator together with the housing at the top. Figure 3 shows the results for the system electronic compartment [7].

Based on values shown in table 1 it has been chosen to place a number of 42 Azur Space 3G30A solar cells on the Rover. Technologies such as CIGS cells or non-crystalline silicon cells also have been investigated, but proved to be disadvantageous in terms of efficiency. The configuration of the panels are 7S1P for the front and

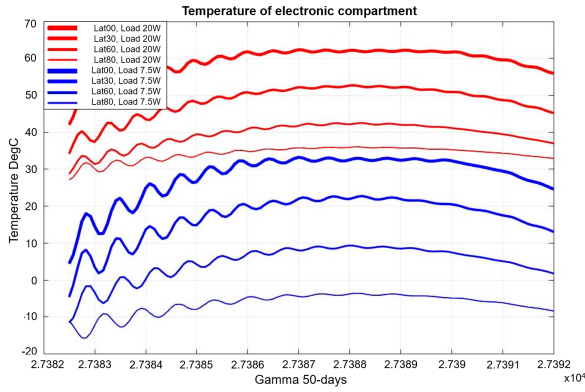


Figure 3. Simulation results for thermal conditions of the rovers electronic compartment. Discrete-time steps were increased for the simulation because of performance reasons what leads to oscillating values at the beginning [7]



Figure 4. Rover MOVE at DFKI Space Exploration Hall

back and 7S2P for the sides. As figure 4 shows, the cells are arranged around the rover body while the top surface is foreseen for a radiator. An aluminium body as mounting frame is used regarding of manufacturing and heat conduction. The colors of the rover do not reflect the final design and were chosen for design reasons.

Although the rovers mass matches with the goal of being in the range of 5 kg the mass budget of the system is not representative, thus some of the components being used from customer market. For example the camera or the radio modules are not equivalent to those suitable for space flight. The EPS balanced it, being much heavier than necessary cause several boards were installed for monitoring or testing. Nevertheless, for giving an impression table 2 gives insight of masses from components being used.

Technology Demonstration In addition to the requirements regarding size, weight, and required power, the main focus in the design of the EPS is on technology demonstration. Therefore, in the chosen design, each functional unit is implemented as a separate board. The design relies entirely on COTS parts, avoiding the use of highly specialized components. For the programmable logic attention was paid to a uniform component choice

Table 2. Mass budgets for the rover MOVE. The total mass of the system is 5.8 kg

Components		Mass
Mechanic	Structure	14%
	Drives with wheels	18%
	Chassis	9%
Electronics	Boards	14%
	Connectors	5%
	Housing	19%
Solar panel		10%
Energy storage		7%
Payload		4%

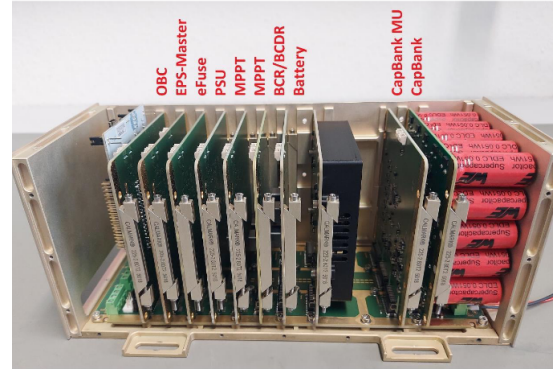


Figure 5. EPS in assembled state. One side panel and the cover removed for illustration.

with low power consumption. The uniform micro controller selection reduces the effort for the firmware development considerably, but it is a compromise since the different functional units have various requirements regarding IO count, computing power, and memory. Figure 5 showing the electronic compartment for the rover used.

3. ELECTRICAL POWER SYSTEM

3.1. General description

The EPS technology demonstrator is divided into individual functions designed as independent modules:

- Batteries (primary, secondary),
- charge and discharge controllers (based on SEPIC converters, implemented with GaN-FETs),
- supercapacitors,
- supercapacitors monitoring unit,
- power supply unit (based on step-down converters),
- power distribution unit with overcurrent protection (eFuse),
- MPPT (based on synchronous step-down converter, implemented with GaN-FETs),
- solar switching shunt regulators,
- EPS master,
- OBC.

Table 3. Overview storage technologies used for the rover. The run time was calculated according to rovers power consumption while moving continuously 1 and 100% DoD

Technology	Cells	Capacity	Mass	Runtime
Li-SOCl2	3x LSH20	140.0 Wh	300 g	6.7 h
LiFePo	3x 18650	14.5 Wh	154 g	50 min
SuperCap	25x WCAP STSC	0.84 Wh	280 g	2 min

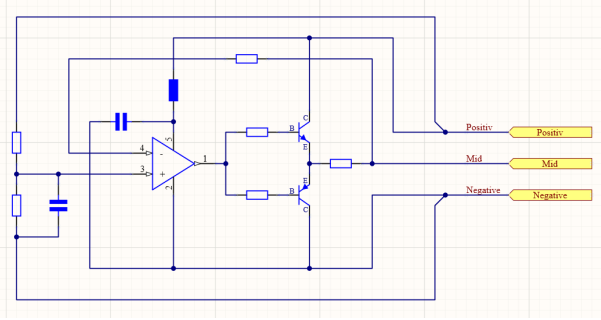


Figure 7. One out of four supercapacitor balancer per module

realised. In order to achieve the widest possible temperature range without loss of electrical performance and a longer lifetime, the maximum voltage of the individual capacitors was limited from 2.7 V nominal (2.85 V surge) to 2.2 V nominal (2.3 V surge). This theoretically allows an operational temperature range of -40 to +85 degree Celsius without any additional reduction in performance. Thus, the electrical storage has a capacity of 50 F at 11 V. Assuming a minimum bus voltage of 5 V allowing to get an electrical charge of 0.66 Ah (equation 3.3).

$$C_{charge} = \frac{((\frac{1}{2} \cdot 50 F \cdot 11 V^2) - (\frac{1}{2} \cdot 50 F \cdot 5 V^2))}{3600 As}$$

Four simple balancers, shown in figure 7, based on op-amps with external current boosted transistors were integrated directly on the supercapacitor module. In addition, an overvoltage protection (Fig. 8) of 2.4 V was provided in parallel to each capacitor group, reacting as soon as the balancing current of the balancer is no longer sufficient. As a further protective feature, 5 potent schottky diodes are connected in parallel to the capacitors to prevent a polarity reversal. Based on datasheet, a single supercapacitor can deliver over 11 A nominal current and over 33 A at peak. The module would therefore be able to deliver theoretically over 50 A nominal and 150 A peak. To limit this, a 10 A fuse is connected between the supercapacitors and the backplane.

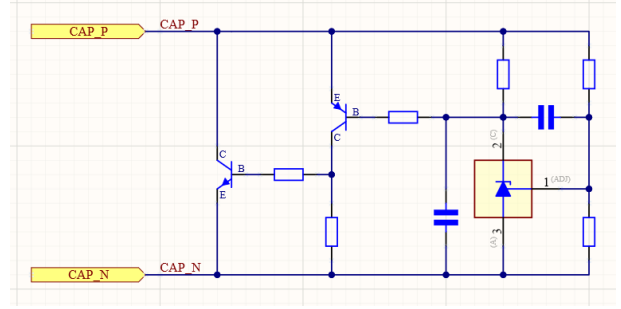


Figure 8. One out of five supercapacitor over voltage protection per module

3.4. Solar controllers

Two different types of solar controllers have been implemented. The first one is a two-channel MPPT converter based on GaN FETs in buck topology, and second is an eight-channel solar shunt switching regulator.

MPPT For the MPPT, two identical synchronous buck controllers based on GaN FETs were used to handle two independent solar panels. The GaN FETs [11] allows high switching frequencies, low power losses as well as high resistance to radiation. Due to the switching frequencies the sizes and volumes of the power inductors and capacitors could be kept at low volume. Current and voltage measurements were implemented on the input and output sides to determine the optimal operating point of the solar panels and to measure the status of the power output to the regulated bus. The control algorithm of the MPPT converters is implemented in the microcontroller used. In addition, there is the an option of operating several of these converters in cold redundancy. For this, a solid-state relay based on two anti-serial P-MOSFETs is connected in front of each of the two MPPT channels. The MPPT converters are designed for up to 60 W per channel. Two of these modules (without additional redundant modules) are used in the current system design where four sides equipped with solar panels.

Solar Shunt Switching Regulator Unlike the MPPT converters, the solar shunt regulator is based on a purely analogue control. A simple Main Error Amplifier (MEA) measures the bus voltage and feeds the error signal into a resistor decade. This is monitored by comparators and gradually switches the individual sections on or off. On a solar shunt regulator module, 8 channels are implemented, each of them is optimized for a single string of triple-junction solar cells. Since the solar panels of the MOVE rover was originally designed for the MPPT method, the shunt controller here achieves an efficiency of about 65% under optimal light conditions. However, with an optimized solar panel, for example with 5 serial cells or an increase in the system voltage, the efficiency could be increased to almost 90%. However, the major

advantages of the shunt regulators are their simplicity due to the absence of complex (programmable) control and highly specialized components, its compactness, and its easy scalability.

3.5. Communication

CAN-Bus CAN bus (2.0B) was chosen as the main interface for data exchange on the backplane as a universal interface in the EPS or between the modules that contain programmable logic. The CAN bus has found its way into many safety-critical industrial areas and has also been standardized for European space travel with the ECSS-E-ST-50-15C. However in the MOVE rover, we implemented the UAVCAN (Uncomplicated Application-level Vehicular Computing and Networking) protocol instead of the OpenCAN software layer from ECSS-E-ST-50-15C. The major reasons to choose UAVCAN were the public availability of the protocol, the good documentation, and quality of the implementation in terms of code quality and test coverage. In order to keep the number of modules in a system variable, the physically necessary termination for the CAN bus is included on the backplane. In this way the termination can be provided at the physically most suitable start and end point. A so-called high-impedance weak termination was provided on each module connected via CAN bus, optimises the EMC behaviour. In addition, TVS diodes and capacitors are used on the bus signals of each module to prevent interfering transients from reaching the transceiver.

LVDS Parallel to the CAN bus, as a replacement or redundancy, a LVDS system in daisy-chain was implemented. However, our experience with the current CAN bus solution relies us to proceed without this extra interface in a redesign or TRL increase. - It is in discussion to have ideally a redundant CAN bus to increase reliability.

EPS Telemetry Interface As depicted in Figure 6 the EPS has its own telemetry interface. The telemetry link is primarily for debugging and monitoring of the EPS to communicate its status to a higher-level system. The Node Level Data Link Communication (NDLCom) protocol [12] was implemented for communication. This is the primary communication protocol developed and used at DFKI for low-level communication in robotic systems.

Discrete Signals Since not all modules have programmable logic and a CAN bus or LVDS interface, additional discrete signals were used to control a restart and power-down from EPS master and giving errors and warning states from slave modules. A dedicated master module orchestrates these discrete signals and tunnels them to the OBC or wirelessly to an external participant or user.

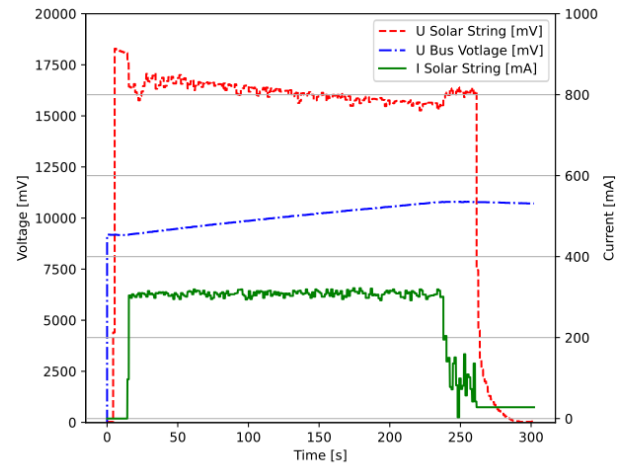


Figure 9. Charging process of the EPS with one solar string controlled with a MPPT module. When the solar string is illuminated, a voltage of over 17.5 V could be measured. As soon as a MPP is found, the EPS is charged with approx. 300 mA in the present experiment. If the maximum allowed bus voltage is reached, the MPPT controller shuts down to prevent an overvoltage of the EPS. After the charging test was completed, the light source was switched off.

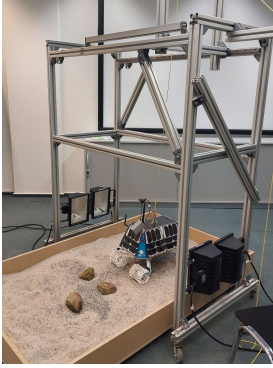
4. EXPERIMENTS

Charging and Discharging of Capbank In laboratory tests, we charged the supercapacitor modules with the maximum expected values of 3 A via laboratory power supply (CC/CV with 3 A / 11 V) and discharged them via electronic load. In this way, a maximum difference of 30 mV observed between the cells in the charged state. If the final charge voltage was still applied for a period of approx. 15 minutes, this drift was reduced to 10 to 15 mV. In a discharge test of 200% of the maximum expected currents, the drift was a maximum of 50 mV. The topology of the balancer, other than typical battery balancers, does not operate a so-called top balancing near the end-of-charge voltage, but permanently targets a balance between the supercapacitors. The drift between the cells was never greater than a maximum of 50 mV, even in the partially discharged state. The drift between the individual supercapacitors becomes smaller the longer a fixed voltage is applied.

This relies us to dispense the separate digital measuring and monitoring unit in the next iteration only relying on the implemented protective elements (balancer, overvoltage protection and polarisation reversal).

MPPT and Shunt Regulator In Figure 9 is depicted the charging procedure of the EPS with one solar string.

Multiple charging tests were carried out in the final phase of the project in the period of January / February. At



(a) Rover MOVE in Testbed. Two floodlights are mounted on both sides. A pulley can be used to compensate gravity.



(b) Rover in simple sun simulator, sun radiation was emulated by halogen floodlights

Figure 10. System testing at laboratory

this time of year, the light yield from daylight in Bremen is not sufficient. Instead, the tests were carried out in the laboratory. Halogen floodlights were used as light sources. Due to the high infrared component, the tests were limited by the heat generated.

System test Testing the system under ideal solar conditions was possible as mentioned before during the duration of the project. Also, due to the corona pandemic situation in February 2022, travelling to a country with better weather conditions for field testing was not possible. This circumstances resulted in the idea to build up quick a testbed for emulating the solar flux under laboratory conditions. Figure 10 shows the rover in there. The halogen floodlights produced only about a half of the power that can be expected under expected light conditions. For completing the scenario we added a simple gravity compensation with pulleys and weights for emulating the lunar gravity conditions. However the testbed was simple, tests were helpful to investigate the interaction of the components on the system level.

Lessons Learned During the system tests with reduced solar irradiation, it appeared that driving only with the CAP bank is possible, but the short runtime makes a proper operation of the system difficult. It was expected that with half of the solar irradiation a stop and go operation would be necessary, but the time to drive with the cap bank itself drops to less than 1 min while charging time increases significantly because of the small surplus. Even better condition can be expected increasing the energy yield, it is desirable from our point of view to be able to drive at least 5 min continuously. This can be achieved only by using the secondary cells or by taking energy from the primary cells.

For the system design it comes to the conclusion that it pays off to reduce the power consumption of the subsystems in every aspect. Especially the power consumption

of the motor controllers should not be underestimated. They are usually installed 4 or 6 times in the system and should not be switched on and off permanently while driving. Increasing in the number of solar cells would be desirable but is limited by the size of the system, which leads to the construction of additional panels.

5. SUMMARY AND OUTLOOK

TRL of the EPS Currently, the TRL of the EPS is in the 3 to 4 range. Based on knowledge we gained, some modules can get additional features or optimizations. Alternative implementations could be done on the existing modules. To increase the TRL to 4 till 6 and beyond, a mission description needs to be clearly defined. Further, equivalent components with radiation tolerance, radiation resistance, or upscreensed parts are need to be identified and deployed for use on the modules. Accordingly, the modules would need to be adapted to the mission profile. The use of an OBC from the CubeSat sector instead of in-house development would also be a worthwhile consideration.

Alternative uses and applications It would be feasible to reuse the EPS for stationary functions in order to create, for example, a stationary relay station, radio beacon or a location-based measuring station. Further development of the modules into the CubSat sector would also be possible. In general, the technology can also be scaled up and used for larger systems.

EPS basic design The configurable backplane approach is highly desirable for future smaller systems. Beyond the design of the EPS other subsystems and components could easily be integrated in the system. For the COTS approach it allows an efficient verification of the single modules itself. However, the chip crisis caused during the project first issues in the procurement process. We assume that due to the lack of availability an identical replica would be difficult to realize. Therefore, our recommendation for future developments is to no longer rely on COTS components at critical points, e.g. for micro controllers. Instead replace them with HiRel parts.

Evaluation of experiments with the system Nevertheless, we see potential applications for the use of supercapacitors in the future. They can be used to reduce the charging and discharging cycles of a secondary system battery and to increase its lifetime. For cold system temperatures ($T < 0^{\circ}C$), they supports significantly the current capabilities of the EPS. This makes the big difference to conventional EPS systems. From our point of view this could be a necessary feature for the development of future walking robots where direct drives arises will increase higher discharge and charging peaks during operation.

Table 4. Overview of the potential use of the storage technologies for future systems, ¹: equal sota 1, ²: small rover $m \leq 5kg$

Application	Solar	P.-Bat.	S.-Bat.	Caps
common ¹ rover design	x		x	
small ² rover without chemical storage	x			x
small rover with emergency power system	x	(x)	(x)	x
single use system			x	x
rover with emergency system and high current output capability	x	x	x	x
legged system	x		x	x
stationary system	x	(x)	(x)	x

Looking at table 3, it is obvious that the energy density of the secondary cells used is very high on comparison, which makes them ideal for a single use system. A combination of the caps and primary cells could be use, to build for example a system for the exploration of small craters, whereby it can be assumed that climbing back the walls becomes impossible for a rover. Also the thermal conditions in a lunar crater which range from about -150 °C to 110 °C would be a reason here to renounce from rechargeable batteries. In such an operational environment, the EPS here designed could exploit its full potential.

To sum up results we gained, table 4 gives an broad overview about the potential use of energy storage technologies in future space applications. Our estimation based on technical experiences we gained from the work in project SEARCH and assumptions from literature review for future lunar exploration.

Further Use The rover MOVE will be used at DFKI for further testing of the EPS and the rovers power setup in field trials. With that knowledge we gained, it is envisioned to tailor the EPS for a future mission. The interrelations between the EPS and the TCS will also to be part of further projects. Increasing the total mass of the system to achieve a suitable design for nightsurvival is conceivable. For this it is planned to build a rover that contains both subsystems as testbed for supporting DFKIs strategic development road map.

ACKNOWLEDGMENT

The authors would like to thank the project SEARCH team and all supporting staff at DFKI Robotics Innovation Center Bremen. Special thanks goes to the Walter Kern GmbH for developing the wheels and chassis of the rover MOVE and also for the manufacturing of the mechanical parts. The work presented is part of the projects SEARCH (grant no. 50RA 2041) which are funded by the German Space Agency (DLR Agentur) with federal funds of the Federal Ministry for Economics Affairs and

Climate Action in accordance with the parliamentary resolution of the German Parliament.

REFERENCES

- [1] John Walker. Flight system architecture of the sorato lunar rover. In *Proceedings of the International Symposium on Artificial Intelligence, Robotics and Automation in Space (i-SAIRAS 2018)*, pages 4–6, 2018.
- [2] Midhun S Menon, Adithya Kothandhapani, Nardhini S Sundaram, Vivek Raghavan, and Sanath Nagaraj. Terrain-based analysis as a design and planning tool for operations of a lunar exploration rover for the teamindus lunar mission. In *SpaceOps Conference*, page 2494, 2018.
- [3] AJ Gerner, JA Cyrus, F Meyen, and JB Cyrus. Advances in lunar science return via distributed instrument mobility and swarm robotics: The lunar outpost mobile autonomous prospecting platform (mapp) rovers. *LPI Contributions*, 2635:5018, 2021.
- [4] Astrobotic Technology. *CubeRover Payload Users Guide v1.7*, 2021.
- [5] Roland Sonsalla, Florian Cordes, Leif Christensen, Thomas Roehr, Tobias Stark, Steffen Planthaber, Michael Maurus, Martin Mallwitz, and Elsa Kirchner. Field testing of a cooperative multi-robot sample return mission in mars analogue environment. In *Proceedings of the 14th Symposium on Advanced Space Technologies in Robotics and Automation (ASTRA-2017)*, 06 2017.
- [6] Toshiki Tanaka, Takuto Oikawa, Keeni Shruti, Teruhito Iida, Kazuya Yoshida, and John Walker. Design and implementation of thermal control strategy for micro-size lunar exploration rover hakuto. In *Proceedings of the 69th International Astronautical Congress (IAC)*, 10 2018.
- [7] Jan Wilke Krahwinkel. Thermal-analyse zur konzepterstellung und evaluieren eines mondrovers. Master's thesis, Hochschule Bremen, 2021.
- [8] Datasheet ept one27. <https://www.ept-connectors.com/index.php?One27--1-27-mm-SMT-connectors,2022>.
- [9] ARTES-ESA: Evaluation of Supercapacitors and Impacts at System Level, 2016. <https://artes.esa.int/projects/evaluation-supercapacitors-and-impacts-system-level>.
- [10] Würth Elektronik. *Datasheet WCAP-STSC Supercapacitors(EDLC's) - 850617022002*, 2022. <https://www.we-online.com/katalog/datasheet/850617022002.pdf>.
- [11] EPC. *Datasheet EPC2055 – Enhancement Mode Power Transistor*, 2020. https://epc-co.com/epc/Portals/0/epc/documents/datasheets/EPC2055_datasheet.pdf.
- [12] M. Zenzes, P. Kampmann, M. Schilling, and T. Stark. Simple Protocol for Heterogeneous Embedded Communication Networks. In *Proc. of the Embedded World Exhibition and Conference*, Nürnberg, Germany, February 2016.